

Identifying Key Physical Properties of Simple Organic Drop Cast Films that give Visible to Ultraviolet Light Up-Conversion

Francesco Lodola,^[a] Hector Miranda-Salinas,^[a] Suman Kuila,^[a] Andrew Danos,^[a, b] and Andrew P. Monkman^{*[a]}

We demonstrate UV-emitting films of 2,5-diphenyloxazole (PPO) sensitised by 3,3'-carbonylbis(7-diethylaminocoumarin) (CBDAC), prepared by simple drop casting with rapid solvent evaporation, giving up-converted emission even at low excitation intensities. The mechanisms of up-conversion and triplet quenching in these films has been studied through time-resolved and steady-state spectroscopy. The CBDAC sensitizer aggregates strongly even at low concentrations, with CBDAC phosphorescence being observed in all films, indicating that many triplet excitons do not transfer to the surrounding PPO

annihilator. Nonetheless, at very low sensitizer concentrations (1:40000 CBDAC:PPO), up-converted PPO UV emission is observed at room temperature which is critically dependent on the film formation conditions. Only in films cast onto substrates held at 60 °C is dominant TTA-UC observed. Comparing to similar sensitised films of TIPS-naphthalene, which are TTA-inactive, we deduce that π -stacking of the PPO, prevented by the TIPS side groups in the TIPS-naphthalene films is crucial for efficient triplet diffusion and up-conversion.

Introduction

Recently, there has been significant attention directed towards alternative approaches that increase the utilization of solar energy, which is the most abundant and clean energy source for the future development of a green society.^[1] For example, UV light with wavelengths less than 400 nm has a wide range of applications,^[2] including photocatalytic water splitting for 'green' hydrogen production^[3-5] and photocatalytic CO₂ reduction to produce chemical fuels.^[6,7] However, such high-energy photons represent only approximately 4% of the solar spectrum,^[8] and so efficient ways to convert visible photons to UV are required to use solar light for these specific purposes at commercial scales.

Triplet-triplet annihilation up-conversion (TTA-UC) is a powerful method for generating shorter-wavelength photons than incident light, incoherently and at low power densities on the order of a few mW/cm² (such as solar radiation).^[9] In TTA-UC, a sensitizer molecule absorbs incident visible photons, forming excited singlet states that rapidly convert into triplet

states via intersystem crossing (ISC). This is followed by triplet energy transfer (TET) from the sensitizer to the (TTA-UC) emitter, that forms long-lived triplet states. As the triplet exciton concentration increases, triplet-triplet annihilation (TTA) becomes possible, leading to the production of a singlet excited states in the emitter which then emits at shorter wavelength than the initial sensitizer excitation. Due to the involvement of long-lived intermediate triplet excited states, molecular properties of the triplet sensitizer can be tuned to exploit the visible solar spectrum.^[10-15] In this way, even the visible photons of solar radiation can be up-converted into useful UV photons.

Even though new molecules for UV TTA-UC are continuously being developed that function well in solution^[2,16,17] including the excellent performance recently demonstrated using TIPS-naphthalene by Harada et al,^[18] in order to ensure safety, stability, long operating lifetimes, and environmentally-friendly routes towards applications, using organic solvents that are volatile, flammable, or bio-toxic should be avoided, requiring solid state alternatives to be devised. TTA-UC is though particularly challenging to achieve in film, as the TTA step relies on diffusion and collisions of triplet excitons, which is typically achieved by molecular diffusion in solvents but requires efficient triplet migration via hopping in solid state.^[19] Nonetheless, solid UC systems are the only viable option for commercial implementation of this technology, which has been extremely difficult to achieve even in research setting.^[20,21] Promisingly, a few successful examples have demonstrated the feasibility of achieving highly efficient emission in solid-state UC systems, at low excitation intensities.^[22-24] Therefore, a deeper understanding of the key physical properties underlying this phenomenon is essential.

Here, we investigate very simple solid films that give UV from sensitised TTA-UC based on metal-free coumarin deriva-

[a] F. Lodola, H. Miranda-Salinas, S. Kuila, A. Danos, A. P. Monkman
OEM research group, Department of Physics, Durham University,
Durham DH1 3LE, United Kingdom
E-mail: a.p.monkman@durham.ac.uk

[b] A. Danos
School of Physical and Chemical Sciences, Queen Mary University of
London, Mile End Road, London E1 4NS, United Kingdom

Supporting information for this article is available on the WWW under
<https://doi.org/10.1002/cptc.202400341>

© 2025 The Author(s). ChemPhotoChem published by Wiley-VCH GmbH. This is an open access article under the terms of the Creative Commons Attribution License, which permits use, distribution and reproduction in any medium, provided the original work is properly cited.

tive, 3,3'-carbonylbis(7-diethylaminocoumarin) (CBDAC) as a sensitizer^[25,26] and dispersing this in the promising annihilator, 2,5-diphenyloxazole (PPO)^[17] as the TTA-UC host material. We specifically investigate drop-cast TTA-UC films, using a simple solution deposition method compatible with commercial upscaling. Spectroscopic techniques reveal key issues with this sensitizer, including phase segregation at moderate concentrations, but also demonstrate the notably advantageous characteristics of PPO as an emitter in bulk film. The CBDAC:PPO films are also compared to films using TIPS-naphthalene as the TTA-UC annihilator and host, which are unable to achieve up-converted emission. Comparison between PPO and TIPS-naphthalene using time resolved spectroscopy and X-ray analysis provide key insight into why PPO alone achieves TTA-UC. Ultimately the CBDAC:PPO system shows several promising features in solid state, effective triplet mobility, and UV up-converted emission even at very low incident powers (~ 0.3 mW/cm²) in simple films, whereas the TIPS-naphthalene films have very poor triplet mobility because the TIPS groups (vital for suppressing aggregation formation in solution) hinder wavefunction overlap between naphthalene cores preventing triplet hopping. Further, we identify naphthalene dimers in the X-ray structure of crystals and time resolved emission reveals red shifted dimer emission which likely act as traps that further localise triplet excitons and reduce mobility. These findings provide a simple pathway forwards for the development of solid-state TTA-UC for harnessing solar energy.

Results and Discussion

We investigated films prepared via drop-casting rather than more complex processes that have recently yielded excellent results,^[24] because drop-casting is a simple and easily reproducible solution deposition method suitable for future commercial upscaling. Full details of film preparation are given in the supporting information.

Up-converting films were drop-cast from toluene solutions (100 μ L) of different sensitizer and annihilator mixtures onto 1 cm² quartz substrates. The process was carried out in air, with the substrates held at room temperature or at a temperature of 60 °C to quickly drive off solvent. This rapid drying was found to be crucial to avoid total phase segregation of the sensitizer and annihilator species, with uniform physical dispersion fundamental for efficient TTA-UC.^[27,28] The well-mixed films also support improved triplet mobility and long-range order compared to those deposited at room temperature, as discussed below.

As shown in Supporting Information Fig.S1, films with a mass ratio of 1:20000 the CBDAC:PPO films exhibit very similar UV emission behaviour to those at 1:40000. At these levels we propose that the increased absorption of incident photons and changes in triplet mobility compensate each other. To understand the general behaviour of the sensitizer and emitter molecules in the drop cast films, steady-state optical measurements were made. TTA-UC films with PPO as the host were compared to non-TTA Zeonex matrix films at the same ratio of 1:40000 (CBDAC:host). Emission spectra are also presented for higher concentration Zeonex and UGH (1,3-Bis(triphenylsilyl)-benzene) films doped at 1:100 with CBDAC, as well as 20 μ M CBDAC solutions in dichloromethane (DCM) and toluene (PhMe) in Figure 1.

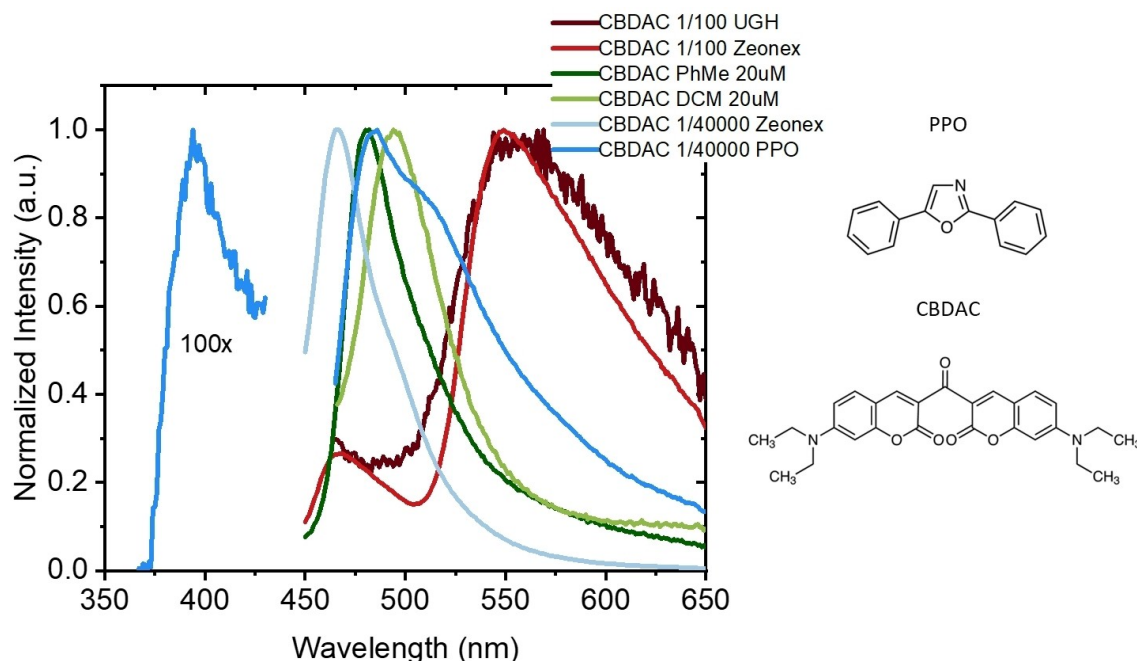


Figure 1. Steady-State emission of CBDAC solution and CBDAC films in PPO, UGH, and Zeonex. Excitation wavelength set at 440 nm to selectively excite the CBDAC sensitizer.

The results obtained (in air at typical fluorimeter excitation intensity of $\sim 0.3 \text{ mW/cm}^2$) show that in the up-converting films (1:40000 CBDAC:PPO, Figure 1) there is detectable UV emission at a shorter wavelength than the excitation wavelength (440 nm), with an intensity ratio of 1 to 100 compared to the fluorescence band of CBDAC around 485 nm. The up-converted UV intensity was found to maximise at between 1:20000 and 1:40000 CBDAC:PPO, Figure S1. The sensitizer fluorescence band in PPO is very broad with a peak at 486 nm (corresponding to the fluorescence band of CBDAC at 20 μM in toluene) and also a second feature around 520–530 nm, as previously observed.^[24] In the CBDAC films in Zeonex (1/40000), the main fluorescence band is observed at 460 nm with a weak vibronic shoulder at ca. 500 nm. Unlike the films with PPO small molecule as host, where the packing is influential, the Zeonex polymer host acts much like a viscous solution. The red shift of approximately 20 nm in the main fluorescence emission peak in the PPO film is hence attributed to the polar character of PPO host interacting with the charge-transfer character of the excited singlet state of CBDAC.^[29,30] This attribution is confirmed by measurement in more polar 20 μM dichloromethane, which exhibits a larger red-shift of the emission band and no vibronic structure.

In Zeonex films doped with a higher level of CBDAC (1:100, Figure 1), the fluorescence band around 465 nm remains, but a new band due to sensitizer phosphorescence is also observed with a peak at 550 nm. This band is also observed in 1:100 films in small molecule matrix UGH. To confirm the nature of the new band in high-sensitizer content films, time-resolved measure-

ments at room temperature were performed on CBDAC samples in Zeonex at 1:100 and 1:40000.

In both films the CBDAC fluorescence band behaves similarly, with a bi-exponential decay, discussed later. The significant difference lies in the phosphorescence band at 550 nm. In films with a low CBDAC content (1:40000, bottom), this band emerges at around 100 μs and exhibits an extremely long-lived signal, which can be observed even up to 30 ms at room temperature. This phosphorescence band maintains the same vibronic structure previously found in solution,^[25] which indicates isolated CBDAC molecules in the polymer matrix. In fact, most of the triplets created on the CBDAC molecules, which have high intersystem crossing (ISC) yield,^[31] have the opportunity to relax non-radiatively at room temperature. Therefore, in steady-state conditions the main band observed is fluorescence, while the remaining triplets, which provide a very weak signal detectable by the iCCD camera, retain the vibronic structure of isolated molecular phosphorescence. This assignment of phosphorescence emission is further supported by measurements at 80 K, in which unambiguous phosphorescence with matching spectrum is observed (*vide infra*).

In films with a high concentration of sensitizer (1:100, Figure 2a), the time-resolved emission is very different. In addition to the CBDAC fluorescence (lifetime 2.5 ns) and later phosphorescence, another band is observed at ca. 530 nm and is present even in the earliest resolvable spectrum (1 ns). By 6 ns this band has comparable intensity to the fluorescence band, maintaining a broad structureless band shape (lifetime 95 ns) typical of aggregate emission. This red band also gives delayed fluorescence with lifetime 700 ns, and is still clearly

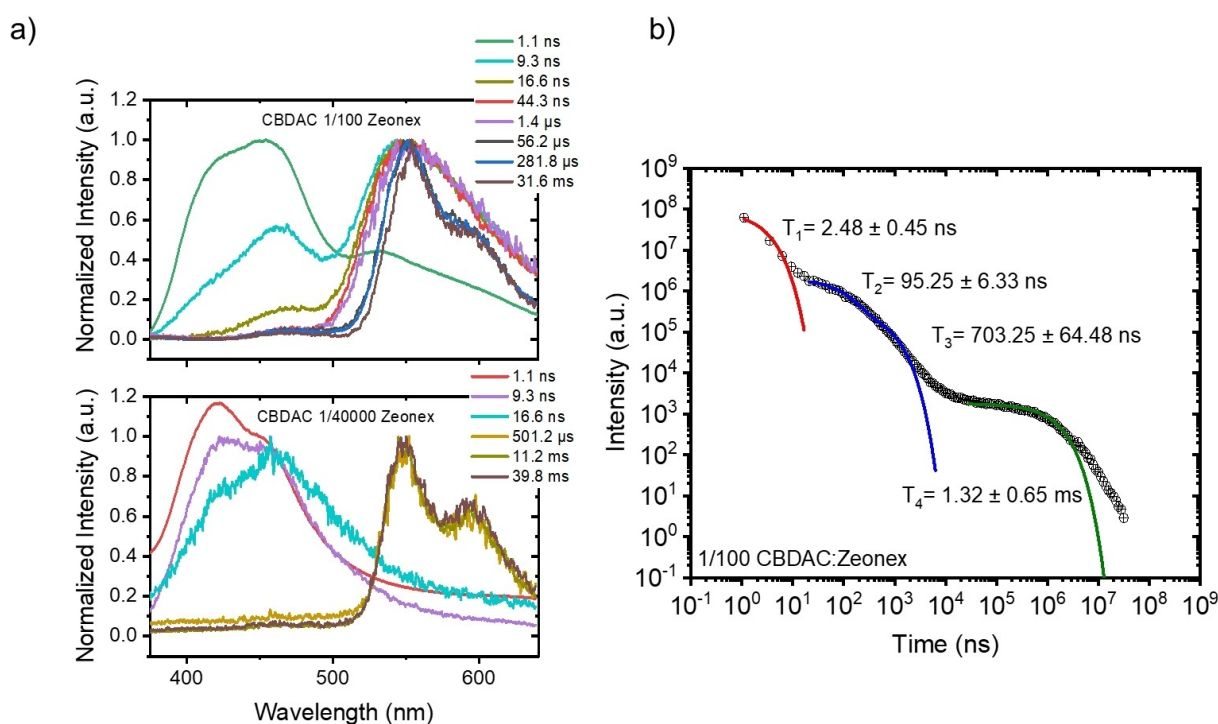


Figure 2. a) Room temperature time-resolved emission spectra of CBDAC doped Zeonex films (1/100 top and 1/40000 bottom) following 355 nm excitation. b) time resolved emission decay of the 1/100 CBDAC:Zeonex film, in the spectral window 520 nm to 600 nm, fitted with exponential functions across different time regions.

present after 2 μ s. In the 100's of microsecond region, the vibronically structured emission band re-emerges, arising from the isolated molecule phosphorescence with lifetime > 1.3 ms. These spectra and kinetics help to explain why films doped with as little as 1:1000 CBDAC fail to demonstrate up-conversion properties. Indeed, we propose that at 'normal' concentrations of sensitizer (higher in comparison to the concentrations used here, favouring greater light absorption) the problem of sensitizer aggregation becomes terminal. Excitation formed on the CBDAC molecules become trapped in CBDAC aggregates and decay radiatively. From the bi-exponential decay of the aggregate emission (Figure 2) we tentatively ascribe the behaviour as prompt (aggregate) emission followed by additional delayed aggregate fluorescence arising from CBDAC TTA within the aggregates. This becomes a major undesirable channel that competes with TET (triplet-triplet energy transfer) to the up-converting host, and we have previously observed poor sensitisation due to analogous aggregate quenching in Pd metalorganic sensitizers for NIR to VIS up-conversion.^[32] In the present work though we are further able to reveal the triplet quenching mechanism in the aggregates from the emission kinetics.

To obtain a more comprehensive understanding of the characteristics of PPO and TIPS-naphthalene as TTA-UC emitters in solid state, time-resolved measurements were conducted at room temperature and at 80 K. Neat PPO film photophysics is shown in Figure 3a, phosphorescence of PPO is seen, along with strong TTA. This is compared with the phosphorescence at low temperature (delay 10 ms/integration time 80 ms) of CBDAC in Zeonex, which is very similar to that previously assigned in solution^[25] and in room temperature films, and in UGH where the phosphorescence exhibits the same vibronic character as CBDAC in Zeonex, but with slight differences

presumably due to different packing, influenced by the small molecule host.

From previous solution studies, CBDAC cannot sensitize PPO due to the emitter T_1 state being higher in energy than the sensitizer T_1 by 200 meV.^[17] However, as we see here, in the solid state this becomes possible due to a red shift of the PPO excited states caused by solid-state π -stacking of the annihilator. A 15 nm red shift in the fluorescence band of PPO, Figure S2, is found (using the red edge of the emission band, to avoid self-absorption effects) when comparing the neat up-converting film with solution/Zeonex measurements. In the PPO film, the PPO triplet is consequently observed ca. 50 meV below that of the CBDAC sensitizer (taking on-set energies) Figure 3a, which allows triplet energy transfer in the films that would not be possible for the isolated dissolved molecules that have higher triplet energies.^[33] This energy gap, 50 meV, at room temperature corresponds to only $\sim 2k_B T$, and so some back transfer can be expected from PPO to CBDAC which may help to explain the CBDAC phosphorescence observed in CBDAC:PPO films. Based on the acceleration of CBDAC phosphorescence emission in inert 1/40000 Zeonex and 1/40000 PPO films, we estimate Dexter transfer rates of 2.2×10^6 and $1.8 \times 10^5 \text{ s}^{-1}$ for films with and without rapid drying (Figures 5a and 5b) respectively. The slower rate of Dexter transfer in the slow-drying film is consistent with its worse TTA performance.

By comparison, TIPS-naphthalene films effectively show no red shift in the PL compared to solution, Figure 4a, but the phosphorescence on-set is at 587 nm so that the triplet energy gap to CBDAC is 250 meV, so little back transfer of triplets is possible and more effective sensitisation should ensue, Figure 4c. However, in TIPS-Naphthalene:UGH (1:100) films we also observe prompt emission at longer time, red shifted, with a structureless band, peak at 430 nm, which we ascribe to TIPS-

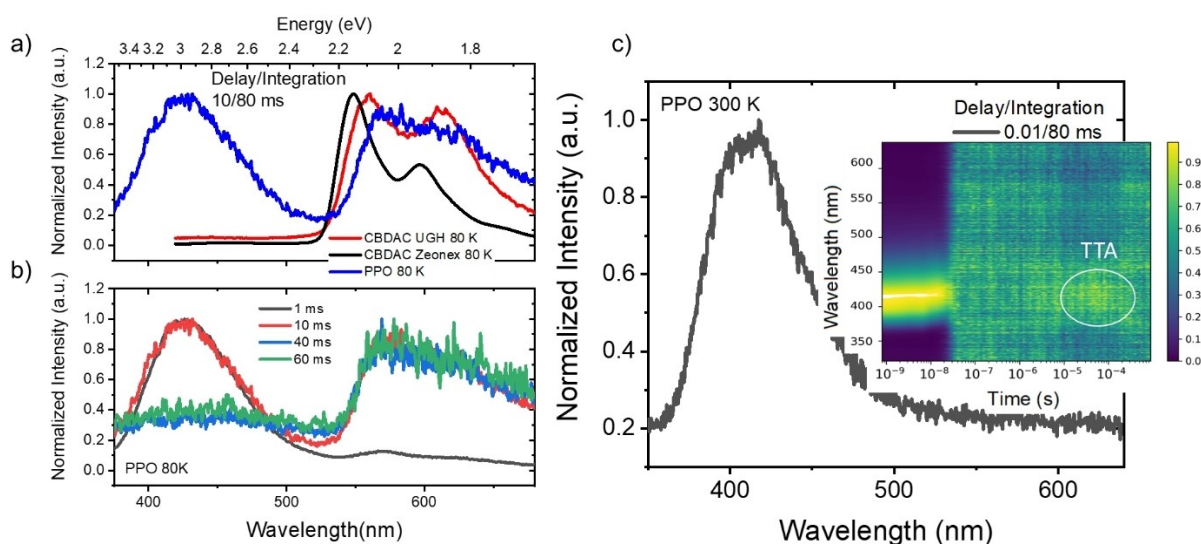


Figure 3. a) 80 K delayed emission spectra of CBDAC in Zeonex and UGH films compared to neat PPO film (delay time 10 ms/ integration time 80 ms). b) 80 K emission spectra of neat PPO film at different delay times. c) Individual time-resolved emission spectrum showing room temperature TTA in neat PPO film observed with long delay and integration times (delay time 0.1 ms/ integration time 80 ms), inset is the 300 K contour plot of neat PPO film.; all spectra obtained using 355 nm excitation.

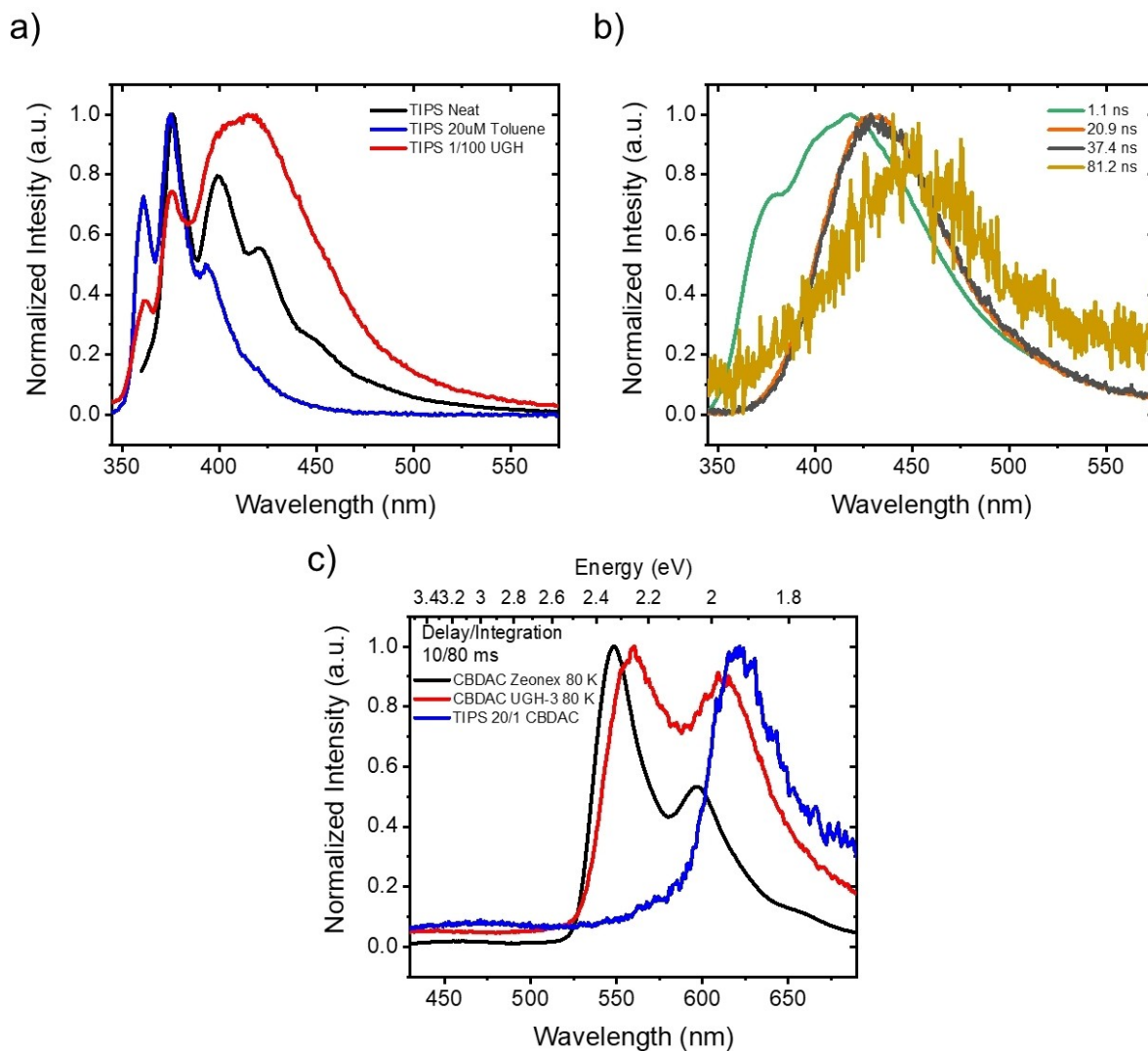


Figure 4. a) TIPS-naphthalene fluorescence spectra measured in toluene solution and in films, both neat and in UGH. b) Time-resolved emission from TIPS-naphthalene 1/100 UGH film. Clear evidence of TIPS-naphthalene dimer emission (peak 430 nm) is observed after fast prompt monomer fluorescence, using 355 nm excitation. c) Phosphorescence measured at 80 K (10 ms delay 80 ms integration) of TIPS-naphthalene:CBDAC (20:1) drop cast film compared to CBDAC phosphorescence measured in Zeonex and UGH films

naphthalene dimer states, Figure 4b, and in neat TIPS-naphthalene films, Figure S3. The latter films also show higher order aggregate emission as well. Comparing the emission of TIPS-naphthalene:UGH (1:100) films which show strong dimer emission, to emission in dilute toluene solution and neat TIPS-naphthalene films, it is clear that neat film has a dimer emission contribution on the red side of the emission band, Figure 4a. The X-ray structure of TIPS-naphthalene crystal, Figure S4, reveals the presence of edge-on TIPS-naphthalene dimers as well as the effective isolation of TIPS-naphthalene monomer (and dimer) by the surrounding TIPS side groups, both contributing to trapping and hindering of triplet exciton migration in film.

Returning to PPO films, in Figure 3b emission spectra of neat PPO film at low temperature are shown at different delay times. These spectra highlight that at ca. 1 ms the main channel for emission is the annihilation of triplets, alongside a very weak

phosphorescence band. This ratio of emission pathways arises because the PPO phosphorescence lifetime is extremely long, while the high mobility afforded by favourable packing and π -stacking in PPO enables rapid formation of TTA pair states – particularly at early times in the decay when triplet exciton densities are highest. At ca. 10 ms, the bands have equal intensity, while at longer delay times of 40 ms and 60 ms, only the phosphorescence signal from triplets that did not undergo annihilation remains. This confirms that the previously reported X-ray structure of PPO^[24] facilitates triplet migration within the film.

Figure 3c shows an inset of the contour plot of the normalised time-resolved emission spectra of the neat PPO film at room temperature, excited with 355 nm light. It is notable that a delayed fluorescence (TTA contribution) is present after 10^{-5} s, as confirmed in the individually collected emission spectrum (80 ms integration and 0.01 ms delay time). This TTA

delayed fluorescence is attributed to PPO triplets which form by ISC on the PPO, indicating good triplet mobility even at room temperature in this annihilator. This band of TTA delayed fluorescence is however not observed in drop cast films where the substrate was not at elevated temperature Figure S5. We suggest that the 60 °C deposition temperature improves the packing of the PPO in the films and increases their long-range order, enhancing the microcrystallinity of the sample and favouring exciton hopping. This triplet mobility is crucial for solid-state TTA, which is a Dexter-type process^[34,35] and must occur via hopping of triplet excitons between fixed molecules, rather than molecular diffusion as in solution TTA. This improved TTA performance for rapidly dried films is further supported by suppression of CBDAC aggregates for films formed this way, and PPO films formed by melt-casting (Figure S6c) show yet greater TTA contribution indicating yet further improvement of triplet mobility. By comparison, TIPS-naphthalene: CBDAC films show no TTA delayed emission at low excitation intensities and only phosphorescence with a very weak TIPS-naphthalene singlet (single molecules and dimers) emission seen at longer times, exciting the ketocoumarin with a 450 nm nanosecond dye laser. In Figure S6, triplet mobility of both neat TTA host is studied in room temperature dropcast and melted films. and even after melting only very weak

monomer emission is observed at longer time in TIPS melted films.

The kinetics of up-converting films, 1:40000 CBDAC:PPO, dropcast at 60 °C, (in Figure 5a and 5b, a comparison between hot and cold dropcast films of both TTA host is shown) were then investigated, exciting the sensitizer with a 450 nm nanosecond dye laser. Figure 5a shows the contour plot of normalised time-resolved emission, that illustrates the dynamics of triplet excitons in different time regions. The decay of CBDAC fluorescence could not be obtained experimentally in this setup, as the overlapping excitation laser saturates the detector up to 10⁻⁷ seconds. Nonetheless, using TCSPC measurements we measured the biexponential decay of the residual CBDAC fluorescence (Figure 5c), with a fast component of lifetime 6 ns and a longer component having a decay time of approximately 40 ns. A similar decay is observed in the CBDAC: Zeonex films (1:40000, Figure S8, which is consistent with the results obtained in Figure 2. The biexponential emission decay is attributed to the presence of multiple conformers and or monomeric and dimeric forms of the sensitizer, which contribute differently to the intrinsic decay of CBDAC fluorescence even at these low concentrations.^[36,37]

Figure 5a and the corresponding emission intensity decay plot (Figure S9a) allows for a better interpretation of the dynamics of triplet excitons formed in the TTA-UC film. Some of

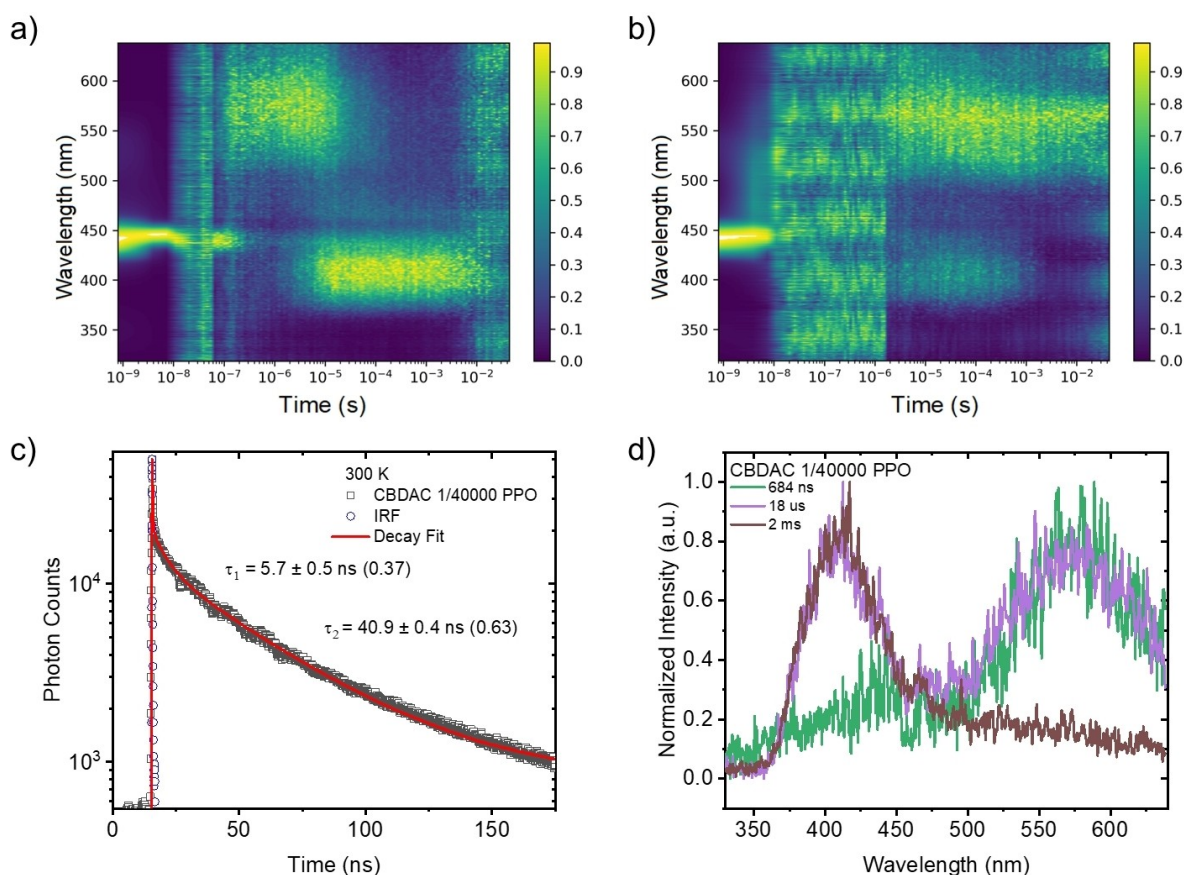


Figure 5. a) hot (substrates heated at 60 °C) and b) cold (unheated substrates) 300 K contour plots of normalised time-resolved emission spectra of CBDAC 1/40000 PPO film (exciting at 450 nm). c) 300 K time-resolved emission decay of fluorescence at 484 nm in CBDAC 1/40000 PPO film, measured by TCSPC. d) 300 K individual emission spectra at different times of hot CBDAC 1/40000 PPO film (exciting at 450 nm).

these excitons are unable to undergo triplet energy transfer (TET) to the PPO emitter and decay, resulting in the phosphorescence band of (isolated) CBDAC at 550 nm following the cessation of 450 nm laser scatter signal. In the region of 1–10 microseconds the phosphorescence band of the sensitizer coexists with a TTA-UC band at shorter wavelength, ca. 400 nm, further seen in Figure 5a and 5d. As we enter the millisecond region, the TTA-UC band remains as the only long-lived emitting band.

It is crucial to note that in an up-converting film made without hot rapid casting, Figure 5b, the TTA-UC band is significantly less intense, and the phosphorescence of the sensitizer continues even in the millisecond region. This once again indicates phase segregation of the sensitizer under these film formation conditions, with excitons trapped in the sensitizer aggregates and hindered exciton transport properties. As mentioned above, comparing the decay kinetics of the residual CBDAC emission reveals an estimated Dexter transfer rate of $1.8 \times 10^5 \text{ s}^{-1}$ for this film, almost ten times lower than for the rapidly dried counterpart. These observations clearly show the necessity of rapid drying and elevated substrate temperature for the casting of the PPO:CBDAC films in order to achieve up-conversion. Comparing the CBDAC:PPO films (Figure 5a), where the TTA-UC is quite intense, to CBDAC:TIPS-naphthalene (Fig. S7 bottom right) films, we observe emission only from the CBDAC and very weak TIPS-naphthalene singlet (dimers and single molecule) emission at relatively long times, $> 10^{-4} \text{ s}$. The timescale of residual CBDAC emission is even longer here, implying even lower Dexter rates from sensitizer to TIPS-naphthalene host. We attribute this behaviour to the solubilising TIPS groups that prevent good wavefunction overlap between the naphthalene cores, preventing effective triplet exciton migration in the film. The observed TIPS-naphthalene dimer emission, in neat and UGH films, also indicates triplet exciton trapping in the films further preventing efficient TIPS-naphthalene TTA-UC. All these findings have been corroborated by measurements using a conventional spectrofluorometer, employing an extremely low incident power ($\sim 0.3 \text{ mW/cm}^2$). In this experimental setup, CBDAC:PPO films exhibited clear up-conversion emission, while CBDAC:TIPS films showed no detectable response in the UV region.

To delve deeper into the solid-state effect within the sensitizer and annihilator, we conducted measurements of their triplet energy levels in both diluted films (1/100 Zeonex) and bulk drop-casted films figure 6. When the molecules are isolated, their triplet energies closely resemble those reported in solution. For instance, in the case of CBDAC, when the molecule is in a dilute film, the triplet energy has an onset energy of 2.36 eV, slightly higher than the 2.33 eV observed in diluted PPO. This proximity in energy levels makes the triplet energy transfer (TET) process feasible. However, upon studying bulk films, a noticeable red shift occurs in both molecules. Bulk films allow molecules to aggregate, resulting in the measured energy level reflecting that of the aggregate.^[33] In this context, CBDAC's triplet energy in bulk films decreases significantly to 2.08 eV, notably lower than its energy in diluted form. PPO exhibits a similar trend, albeit with a less pronounced energy

shift, with an onset energy of 2.26 eV. As depicted in Figure 6b, it is evident that an isolated sensitizer is necessary to facilitate TET. When the sensitizer aggregates, the energy level decreases to a point where TET to the annihilator becomes an uphill process, to reach the triplet energy levels of PPO. Thus, controlling film formation and sensitizer concentration becomes crucial in ensuring effective triplet energy transfer.

Conclusions

In summary, we have demonstrated TTA-UC UV-emitting films consisting of 2,5-diphenyloxazole (PPO) sensitised by 3,3'-carbonylbis(7-diethylaminocoumarin) (CBDAC), prepared using a simple drop casting deposition method. Strong CBDAC phosphorescence is observed in many films, indicating that many triplets remain trapped on the sensitizer and are unable to undergo TET into the emitter. This presents an ongoing challenge towards developing high-performance TTA-UC UV emissive films and could be made worse by the small triplet energy difference between sensitizer and host (50 meV). The CBDAC sensitizer exhibits a strong tendency for phase segregation and aggregation even at very low concentrations. Addressing this is a clear pathway towards improving solid-state TTA-UC performance. At 'high' sensitizer concentrations (which might elsewhere be considered low or normal) we observe CBDAC aggregate fluorescence along with aggregate delayed TTA fluorescence, which effectively quenches the sensitizer triplet population leading to relatively poor sensitisation of the PPO. At very low sensitizer concentrations (1:40,000 CBDAC:PPO) delayed PPO UV emission from TTA is observed at room temperature, even at very low sensitizer excitation intensities in a normal spectrofluorometer. Only in films cast onto substrates held at 60 °C do we observe dominant TTA-UC though, indicating the key role of beneficial π -stacking and triplet mobility to support TTA in these films. While TIPS-naphthalene which gives rise to strong TTA-UC in solution, we find that the solubilising TIPS groups here prevent good wavefunction overlap between the naphthalene cores, preventing effective triplet exciton migration. We also observed TIPS-naphthalene dimer emission which indicates triplet exciton trapping in the films, further preventing efficient TIPS-naphthalene TTA-UC in the solid state.

Author Contributions

F.L. H.M.-S., A.D., undertook the optical and time-resolved spectroscopy measurements. S.K. synthesised and purified materials, A.M. devised the research and supervised the work. F.L. H.M.-S., A.D and A.M. undertook the data analysis, and wrote the manuscript.

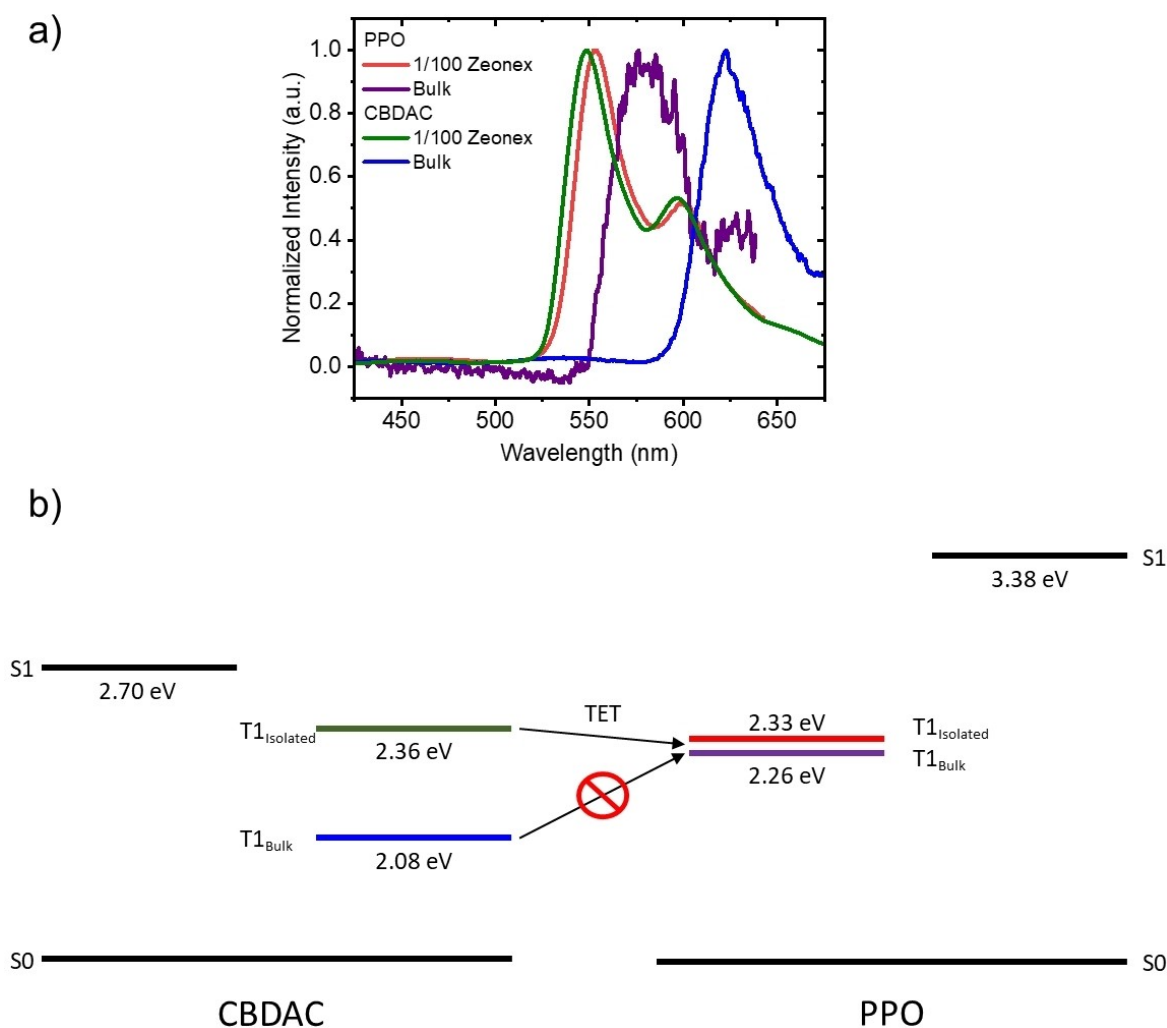


Figure 6. a) Phosphorescence spectra of PPO and CBDAC in diluted (1/100) Zeonex and drop casted bulk film (excitation 355 nm) and b) schematic Jablonski diagram showing the energy levels involved in the triplet energy transfer process, energy taken from the spectral on set.

Acknowledgements

Andrew Monkman, Suman Kuila and Andrew Danos thanks the Engineering and Physical Sciences Research Council (EPSRC) for funding (Grant EP/T02240X/1). Francesco Lodola thanks the EU Erasmus scheme and Parma University for financial support. Hector Miranda-Salinas acknowledges the Mexican National Council for Science and Technology, CONACYT for his student-ship (2019-000021-01EXTF-00308). The authors also thank Dr. Paul McGonigal for supplying an initial batch of TIPS-naphthalene.

Conflict of Interests

The authors declare no competing financial interest.

Data Availability Statement

The data that support the findings of this study are available from the corresponding author upon reasonable request.

Keywords: VIS-UV up-conversion · triplet annihilation · triplet energy transfer · UV photogeneration

- [1] Climate Change 2022: Mitigation of Climate Change, <https://www.ipcc.ch/report/ar6/wg3/>, (accessed 13 October 2023).
- [2] M. Uji, T. J. B. Zähringer, C. Kerzig, N. Yanai, *Angew. Chem. Int. Ed.* **2023**, *62*, e202301506.
- [3] T. Takata, J. Jiang, Y. Sakata, M. Nakabayashi, N. Shibata, V. Nandal, K. Seki, T. Hisatomi, K. Domen, *Nature* **2020**, *581*, 411–414.
- [4] H. Nishiyama, T. Yamada, M. Nakabayashi, Y. Maehara, M. Yamaguchi, Y. Kuromiya, Y. Nagatsuma, H. Tokudome, S. Akiyama, T. Watanabe, R. Narushima, S. Okunaka, N. Shibata, T. Takata, T. Hisatomi, K. Domen, *Nature* **2021**, *598*, 304–307.
- [5] H. Song, S. Luo, H. Huang, B. Deng, J. Ye, *ACS Energy Lett.* **2022**, *7*, 1043–1065.
- [6] A. Behera, A. K. Kar, R. Srivastava, *Mater. Horiz.* **2022**, *9*, 607–639.

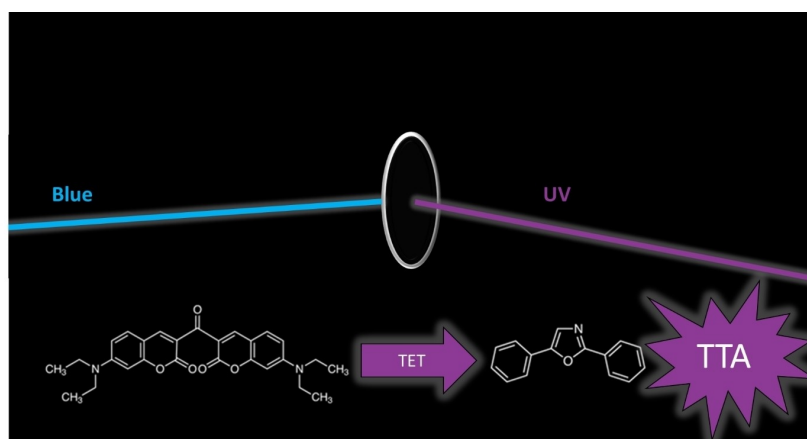
- [7] Y. Xu, S. Wang, J. Yang, B. Han, R. Nie, J. Wang, J. Wang, H. Jing, *Nano Energy* **2018**, *51*, 442–450.
- [8] Reference Air Mass 1.5 Spectra | Grid Modernization | NREL, <https://www.nrel.gov/grid/solar-resource/spectra-am1.5.html>, (accessed 13 October 2023).
- [9] R. W. MacQueen, Y. Y. Cheng, A. N. Danos, K. Lips, T. W. Schmidt, *RSC Adv.* **2014**, *4*, 52749–52756.
- [10] S. Balushev, T. Miteva, V. Yakutkin, G. Nelles, A. Yasuda, G. Wegner, *Phys. Rev. Lett.* **2006**, *97*, 143903.
- [11] T. N. Singh-Rachford, F. N. Castellano, *Coord. Chem. Rev.* **2010**, *254*, 2560–2573.
- [12] A. Monguzzi, R. Tubino, S. Hoseinkhani, M. Campione, F. Meinardi, *Phys. Chem. Chem. Phys.* **2012**, *14*, 4322–4332.
- [13] Y. Murakami, K. Kamada, *Phys. Chem. Chem. Phys.* **2021**, *23*, 18268–18282.
- [14] A. Danos, R. W. MacQueen, Y. Y. Cheng, M. Dvořák, T. A. Darwish, D. R. McCamey, T. W. Schmidt, *J. Phys. Chem. Lett.* **2015**, *6*, 3061–3066.
- [15] A. J. Carrod, V. Gray, K. Börjesson, *Energy Environ. Sci.* **2022**, *15*, 4982–5016.
- [16] T. J. B. Zähringer, J. A. Moghtader, M. Bertrams, B. Roy, M. Uji, N. Yanai, C. Kerzig, *Angew. Chem. Int. Ed.* **2023**, *62*, e202215340.
- [17] A. Olesund, J. Johnsson, F. Edhborg, S. Ghasemi, K. Moth-Poulsen, B. Albinsson, *J. Am. Chem. Soc.* **2022**, *144*, 3706–3716.
- [18] N. Harada, Y. Sasaki, M. Hosoyamada, N. Kimizuka, N. Yanai, *Angew. Chem. Int. Ed.* **2021**, *60*, 142–147.
- [19] S. Mattiello, A. Danos, K. Stavrou, A. Ronchi, R. Baranovski, D. Florenzano, F. Meinardi, L. Beverina, A. Monkman, A. Monguzzi, *Adv. Opt. Mater.* **2024**, *12*, 2401597.
- [20] V. Gray, K. Moth-Poulsen, B. Albinsson, M. Abrahamsson, *Coord. Chem. Rev.* **2018**, *362*, 54–71.
- [21] S. Ráisis, O. Adomeniene, P. Adomenas, A. Rudnick, A. Kohler, K. Kazlauskas, *J. Phys. Chem. C* **2021**, *125*, 3764–3775.
- [22] R. Enomoto, M. Hoshi, H. Oyama, H. Agata, S. Kurokawa, H. Kuma, H. Uekusa, Y. Murakami, *Mater. Horiz.* **2021**, *8*, 3449–3456.
- [23] P. Bi, T. Zhang, Y. Guo, J. Wang, X. W. Chua, Z. Chen, W. P. Goh, C. Jiang, E. E. M. Chia, J. Hou, L. Yang, *Nat. Commun.* **2024**, *15*, 5719.
- [24] R. Enomoto, Y. Murakami, *J. Mater. Chem. C* **2023**, *11*, 1678–1683.
- [25] M. Uji, N. Harada, N. Kimizuka, M. Saigo, K. Miyata, K. Onda, N. Yanai, *J. Mater. Chem. C* **2022**, *10*, 4558–4562.
- [26] J. B. Borak, D. E. Falvey, *Photochem. Photobiol. Sci.* **2010**, *9*, 854–860.
- [27] K. Kamada, Y. Sakagami, T. Mizokuro, Y. Fujiwara, K. Kobayashi, K. Narushima, S. Hirata, M. Vacha, *Mater. Horiz.* **2017**, *4*, 83–87.
- [28] A. Abulikemu, Y. Sakagami, C. Heck, K. Kamada, H. Sotome, H. Miyasaka, D. Kuzuhara, H. Yamada, *ACS Appl. Mater. Interfaces* **2019**, *11*, 20812–20819.
- [29] P. L. Dos Santos, J. S. Ward, M. R. Bryce, A. P. Monkman, *J. Phys. Chem. Lett.* **2016**, *7*, 3341–3346.
- [30] P. Sudhakar, S. Kuila, K. Stavrou, A. Danos, A. M. Z. Slawin, A. Monkman, E. Zysman-Colman, *ACS Appl. Mater. Interfaces* **2023**, *15*, 25806–25818.
- [31] D. P. Specht, P. A. Martic, S. Farid, *Tetrahedron* **1982**, *38*, 1203–1211.
- [32] V. Jankus, E. W. Snedden, D. W. Bright, V. L. Whittle, J. A. G. Williams, A. Monkman, *Adv. Funct. Mater.* **2013**, *23*, 384–393.
- [33] I. A. Wright, A. Danos, S. Montanaro, A. S. Batsanov, A. P. Monkman, M. R. Bryce, *Chem. Eur. J.* **2021**, *27*, 6545–6556.
- [34] D. L. Dexter, L. F. H. Bovey, *J. Chem. Phys.* **1953**, *21*, 836–850.
- [35] A. Monguzzi, R. Tubino, F. Meinardi, *Phys. Rev. B* **2008**, *77*, 155122.
- [36] M. Tasiar, D. T. Gryko, D. J. Pielacmska, A. Zanelli, L. Flamign, *Chem. Asian J.* **2010**, *5*, 130–140.
- [37] R. Nazir, P. Danilevicius, A. I. Ciuciu, M. Chatzinikolaidou, D. Gray, L. Flamigni, M. Farsari, D. T. Gryko, *Chem. Mater.* **2014**, *26*, 3175–3184.

Manuscript received: October 11, 2024

Revised manuscript received: January 14, 2025

Accepted manuscript online: January 16, 2025

Version of record online: ■■■, ■■■



Simple dropcast films demonstrate up-conversion emission from blue to ultraviolet. The low concentration of the sensitizer CBDAC and the π -stacking of the annihilator PPO –

prevented by the TIPS side groups in the TTA-inactive TIPS-naphthalene films – are crucial for efficient triplet diffusion and up-conversion.

*F. Lodola, H. Miranda-Salinas, S. Kuila, A. Danos, A. P. Monkman**

1 – 10

Identifying Key Physical Properties of Simple Organic Drop Cast Films that give Visible to Ultraviolet Light Up-Conversion

